

Templating Effects on the Mineralization of Layered Inorganic Compounds: (1) Density Functional Calculations of the Formation of Single-Layered Magnesium Hydroxide as a Brucite Model

Hisako Sato,^{*,†,‡} Akihiro Morita,[§] Kanta Ono,^{‡,||} Haruyuki Nakano,[⊥]
Noboru Wakabayashi,[†] and Akihiko Yamagishi^{†,‡}

Department of Earth and Planetary Science, Graduate School of Science, The University of Tokyo, Tokyo 113-0033, Japan, CREST, Japan Science and Technology Corporation, Japan, Department of Chemistry, Graduate School of Science, Kyoto University, Kyoto 606-8502, Japan, High Energy Accelerator Research (KEK) Organization, Institute of Materials Structure Science, Tsukuba 305-0801, Japan, and Department of Applied Chemistry, Graduate School of Engineering, The University of Tokyo, Tokyo 113-8656, Japan

Received March 30, 2003. In Final Form: May 21, 2003

This work aims at understanding the formation and stability of a layered structure of brucite mineral $[\text{Mg}(\text{OH})_2]$ via density functional calculations. Because Mg–O–Mg bond formation from a hydrolyzed species of Mg(II) ion is a critical elemental step of mineralization, we studied the reaction mechanism of Mg–O–Mg linkage using a model cluster, $[\text{Mg}(\text{OH})_2]_n$ ($n = 1-10$), in the gas phase and a water solution. The results indicate that no barrier exists during the reaction path from $[\text{Mg}(\text{OH})_2]_{n-1} + \text{Mg}(\text{OH})_2$ to $[\text{Mg}(\text{OH})_2]_n$ with no significant solvent effect of water. It has been confirmed that this polymerization reaction leads spontaneously to a planar cluster, which is regarded as a part of the brucite layer. The results suggest that the layered structure of brucite is a natural consequence of polymerization. These findings will be utilized to establish microscopic modeling for studying a templating effect on the formation of an inorganic thin film.

Introduction

There has recently been an increasing interest in applications of inorganic thin films to functional materials, such as sensors, electrode modifiers, and electronic devices.^{1–3} To synthesize these films, a number of methods have been applied, including the Langmuir–Blodgett method, self-assembly, and alternative deposition.^{4–7} One of the most promising methods is to use an organic floating monolayer as a template for the growth of a layered inorganic compound from an aqueous solution. The rate and orientation of the crystal growth are controlled under the influence of well-ordered functional groups in the template. The main efforts have been focused on clarifying such an effect from the viewpoint of structural consistency between a template and a growing crystal plane.^{8–13}

We have extensively applied this method, namely, the templating method, to layered double hydroxides (LDHs) for a number of reasons, as are described below. LDHs consist of edge-sharing octahedra of a mixture of di- and trivalent metal ions with anions intercalated between layered sheets.¹⁴ They provide a prospective class of materials in several technological fields, such as polymer fillers, medical uses, and precursors of bimetallic catalysts.¹⁵ Although most of the applications of LDHs have been done in the form of a powder state, thin films of LDHs are thought to be a potentially useful material for modifying a solid surface.¹⁶ For the purpose of developing thin films of such layered hydroxides, we have attempted mineralization under a floating monolayer of stearic acid on an aqueous solution of $\text{Mg}(\text{NO}_3)_2$ or $\text{Al}(\text{NO}_3)_3$ at $\text{pH} = 10.5$.¹⁷ As a result, stearate anions acted as an efficient template for the crystallization of both Mg–Al–LDH and brucite at the air–water interface. In the case of Mg–Al–LDH in particular, a thin crystal with a size larger than 5 nm could be prepared within a few hours, whereas other conventional methods, such as homogeneous precipitation, take several months to grow an equivalent size

* Author to whom correspondence should be addressed. Telephone: +81-3-5841-4553. Fax: +81-3-5841-4553. E-mail: h-sato@gbs.eps.s.u-tokyo.ac.jp.

[†] Department of Earth and Planetary Science, The University of Tokyo.

[‡] Japan Science and Technology Corporation.

[§] Department of Chemistry, The University of Tokyo.

^{||} Institute of Materials Structure Science.

[⊥] Department of Applied Chemistry, The University of Tokyo.

(1) Umemura, Y.; Yamagishi, A.; Schoonheydt, R.; Persoons, A.; De Schryver, F. *J. Am. Chem. Soc.* **2002**, *124*, 992.

(2) Xinag, Y.; Villemure, G. *J. Phys. Chem.* **1996**, *100*, 7143.

(3) Fukuda, N.; Mitsuiishi, M.; Aoki, M.; Miyashita, T. *J. Phys. Chem. B* **2002**, *106*, 7048.

(4) Petty, M. C. *Langmuir–Blodgett Films: An Introduction*; Cambridge University Press: New York, 1996.

(5) Feldheim, D. L.; Keating, C. D. *Chem. Soc. Rev.* **1998**, *27*, 1.

(6) Decher, G. *Science* **1997**, *277*, 1232.

(7) Kaschak, D. M.; Mallouk, T. E. *J. Am. Chem. Soc.* **1996**, *118*, 4222.

(8) Britt, D. W.; Hofmann, U. G.; Mobius, D.; Hell, S. W. *Langmuir* **2001**, *17*, 3757.

(9) Xu, G.; Yao, N.; Aksay, I. A.; Groves, J. T. *J. Am. Chem. Soc.* **1998**, *120*, 11977.

(10) Orme, C. A.; Noy, A.; Wierzbick, A.; McBride, M. T.; Grantham, M.; Teng, H. H.; Dove, P. M.; De Yoreo, J. J. *Nature* **2000**, *411*, 775.

(11) Teng, H. H.; Dove, P. M.; Orme, C. A.; De Yoreo, J. J. *Science* **1998**, *282*, 724.

(12) Berman, A.; Ahn, D. J.; Lio, A.; Salmeron, M.; Reichert, A.; Charych, D. *Science* **1995**, *269*, 515.

(13) Aizenberg, J.; Black, A. J.; Whitesides, G. M. *J. Am. Chem. Soc.* **1999**, *121*, 4500.

(14) Miyata, S. *Clays Clay Minerals* **1983**, *31*, 305.

(15) Kaguya, W.; Hessian, Z.; Jones, W. *Inorg. Chem.* **1996**, *35*, 5970.

(16) Roto, R.; Villemure, G. *J. Electroanal. Chem.* **2002**, *527*, 123.

(17) He, J. X.; Yamashita, S.; Jones, W.; Yamagishi, A. *Langmuir* **2002**, *18*, 1580.

of the crystal. To understand the mechanism of the observed templating effect on mineralization, it is highly desirable to understand the structural linkage between a templating monolayer and a growing mineral crystal.

In the present work, we have performed a theoretical study on the mechanisms leading to the layered structure of magnesium hydroxide (brucite). There are some theoretical works of minerals by a similar approach reported.^{18,19} Brucite was chosen as the first model system of our theoretical investigation because it includes only one kind of metal ion [Mg(II)], in contrast to other multicomponent LDHs, which greatly simplifies the identification of the crystal structure. We performed density functional calculations on the polymerization of Mg–O–Mg linkages in brucite as a critical elemental reaction step in crystal growth within the cluster approach. There are some previous theoretical works on the structural properties of brucite by the periodic ab initio calculations.^{20–25} These studies assume the layered structure of brucite to be a prerequisite of the calculations. On the basis of that assumption, structural parameters such as lattice constants, vibrational properties, and elastic constants are predicted and compared with the experimental data.

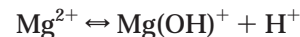
In our attempt, we first determined the most probable hydrolyzed monomer of the Mg(II) ion and, thereafter, elucidated the formation mechanism of the layered structure of brucite through the polymerization of such a hydrolyzed Mg(II) species. A similar theoretical study is reported in the case of Al(III) in zeolite.²⁶ In that study, the structure of a hydrolyzed Al(III) ion is determined theoretically as a partial structure of zeolite. For that purpose, the stability of a coordination structure around Al(III) is compared between the tetrahedral and the octahedral coordinations. Calculation is not extended, however, to the formation of the zeolite framework by the polymerization of such a hydrolyzed Al(III) species. In contrast to this work, our work is to generate a layered structure of brucite by combining monomeric hydrolyzed Mg(II) species. This is an extension of the previous studies on the stability of a single layer of a clay mineral to a simpler layered mineral.^{27,28}

Results and Discussion

(I) Formation Mechanism of a Linked Dimer, [Mg(OH)₂]₂. *General Calculation Model.* Density functional theory (DFT) calculations were performed with the Gaussian 98 program,²⁹ using the B3LYP functional³⁰ in combination with the 6-31G(d) basis set.³¹ When the calculations were performed in a water solution, a solvent

effect was incorporated by a polarizable continuum model (PCM) developed by Miertus and Tomasi³² with 500 points/sphere and a dielectric constant of 78.39.

Structure of a Hydrolyzed Mg(II) Species at a Higher pH Region. To determine the chemical species of Mg(II) at a higher pH region, pH titration was carried out by adding a NaOH standard solution (0.1 M) to an aqueous Mg(NO₃)₂ solution (0.0117 M). At pH = 8–11, the titration curve was analyzed by assuming the following reactions:



On the basis of this scheme, the following expression was derived:

$$K_{\text{sp}}(2/[\text{OH}^-] + b) = a[\text{OH}^-] \quad (1a)$$

$$K_{\text{sp}} = [\text{Mg}^{2+}][\text{OH}^-]^2 \quad (1b)$$

$$a = [\text{NO}_3^-] + [\text{OH}^-] - [\text{Na}^+] - [\text{H}^+] \quad (1c)$$

$$b = K_a/K_w \quad (1d)$$

$$K_a = [\text{Mg}(\text{OH})^+][\text{H}^+]/[\text{Mg}^{2+}] \quad (1e)$$

$$K_w = [\text{H}^+][\text{OH}^-] \quad (1f)$$

where K_{sp} denotes the solubility product of Mg(OH)₂ and K_a is the equilibrium constant for the acid hydrolysis of Mg(II). From a plot of $a/[\text{OH}^-]$ against $1/[\text{OH}^-]$, K_{sp} and K_a were obtained to be $5.4 \times 10^{-10} \text{ M}^3$ and $7.3 \times 10^{-14} \text{ M}$, respectively. On the basis of this, a partially hydrolyzed species, Mg(OH)⁺, was found to be present in a negligible amount [$<0.2\%$ of the total Mg(II) ions] at pH 10.

Stability of Monomeric Mg(OH)₂(H₂O)₄. In the previous experiment,¹⁷ a brucite crystal was found to form under a stearate monolayer at about pH = 10.5. On the basis of this fact, the present calculations modeled a polymerization reaction under this pH condition. According to the titration experiment in the above section, the amount of a partially hydrolyzed species of Mg(II), [Mg(OH)]⁺, was negligible at this pH region. This implies that two protons are dissociated simultaneously from a hydrated Mg(II) ion above pH = 10 and that a predominant reactant of the polymerization reaction is Mg(OH)₂, although it was unknown how many H₂O molecules are coordinated to the Mg(II) ion.

We determined the geometry of a reactant, Mg(OH)₂, by DFT calculations for use in the following sections. In

(18) Hirva, P.; Tikka, H.-K. *Langmuir* **2002**, *18*, 5002.

(19) Pelmenchikov, A.; Strandh, H.; Pettersson, L. G. M.; Leszczynski, J. *J. Phys. Chem. B* **2000**, *104*, 5779.

(20) Baranek, Ph.; Lichanot, A.; Orlando, R.; Dovesi, R. *Chem. Phys. Lett.* **2001**, *340*, 362.

(21) Masini, P.; Bernasconi, M. *J. Phys.: Condens. Matter* **2002**, *14*, 4133.

(22) D'Arco, P.; Causà, M.; Roetti, C.; Silvi, B. *Phys. Rev. B* **1993**, *47*, 3522.

(23) Kruger, M. B.; Williams, Q.; Jeanloz, R. *J. Chem. Phys.* **1989**, *91*, 5910.

(24) Raugel, S.; Silvestrelli, P. L.; Parrinello, M. *Phys. Rev. Lett.* **1999**, *83*, 2222.

(25) Trave, A.; Selloni, A.; Goursoot, A.; Tichit, D.; Weber, J. *J. Phys. Chem. B* **2002**, *106*, 12291.

(26) Ruiz, J. M.; McAdon, M. H.; Garces, J. M. *J. Phys. Chem. B* **1997**, *101*, 1733.

(27) Sato, H.; Yamagishi, M.; Kato, S. *J. Am. Chem. Soc.* **1992**, *114*, 10933.

(28) Sato, H.; Yamagishi, M.; Kawamura, K. *J. Phys. Chem. B* **2001**, *105*, 7990.

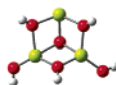
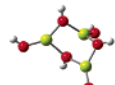
(29) Frisch, M. J.; Trucks, G. W.; Schlegel, H. B.; Scuseria, G. E.; Robb, M. A.; Cheeseman, J. R.; Zakrzewski, V. G.; Montgomery, J. A., Jr.; Stratmann, R. E.; Burant, J. C.; Dapprich, S.; Millam, J. M.; Daniels, A. D.; Kudin, K. N.; Strain, M. C.; Farkas, O.; Tomasi, J.; Barone, V.; Cossi, M.; Cammi, R.; Mennucci, B.; Pomelli, C.; Adamo, C.; Clifford, S.; Ochterski, J.; Petersson, G. A.; Ayala, P. Y.; Cui, Q.; Morokuma, K.; Malick, D. K.; Rabuck, A. D.; Raghavachari, K.; Foresman, J. B.; Cioslowski, J.; Ortiz, J. V.; Stefanov, B. B.; Liu, G.; Liashenko, A.; Piskorz, P.; Komaromi, I.; Gomperts, R.; Martin, R. L.; Fox, D. J.; Keith, T.; Al-Laham, M. A.; Peng, C. Y.; Nanayakkara, A.; Gonzalez, C.; Challacombe, M.; Gill, P. M. W.; Johnson, B. G.; Chen, W.; Wong, M. W.; Andres, J. L.; Head-Gordon, M.; Replogle, E. S.; Pople, J. A. *Gaussian 98*, Revision A.11; Gaussian, Inc.: Pittsburgh, PA, 1998.

(30) Becke, A. D. *J. Chem. Phys.* **1993**, *98*, 5648.

(31) Petersson, G. A.; Al-Laham, M. A. *J. Chem. Phys.* **1991**, *94*, 6081.

(32) Miertus, S.; Tomasi, J. *Chem. Phys.* **1982**, *65*, 239.

Table 1. Optimized Structure of Isomers Including Three Mg Atoms^a

Optimized cluster from a dimer and a monomer	(a) trimer product	(b) trimer-isomer
		
ΔE (eV)	0	+0.0196
No. of OH's at three-centered bridging positions	1	0
No. of OH's at two-centered bridging positions	3	3
No. of OH's at terminal edges	2	3

^a ΔE = total optimized energy; optimized energy (trimer-product).

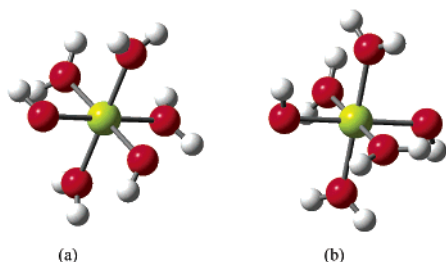


Figure 1. Initial structures of *cis*- and *trans*- $\text{Mg}(\text{OH})_2(\text{H}_2\text{O})_4$: (a) *cis*- $\text{Mg}(\text{OH})_2(\text{H}_2\text{O})_4$; (b) *trans*- $\text{Mg}(\text{OH})_2(\text{H}_2\text{O})_4$.

the neutral pH region, a hydrated state of the Mg(II) ion is reported to be $[\text{Mg}(\text{H}_2\text{O})_6]^{2+}$.³³ We, thus, performed geometry optimization for a six-coordinated structure of $\text{Mg}(\text{OH})_2(\text{H}_2\text{O})_4$, including four water molecules in the first solvation shell. Geometry optimization started with two initial structures, that is, *cis*- and *trans*- $\text{Mg}(\text{OH})_2(\text{H}_2\text{O})_4$ molecules, as are shown in Figure 1. In either case, it led to a stable structure of a $\text{Mg}(\text{OH})_2$ molecule with two OH groups at the *trans* position, while four water molecules did not form stable coordination to the Mg(II) ion. These H_2O molecules provide just a solvating field. Another geometry optimization was carried out for $\text{Mg}(\text{OH})_2$ in a water solution using the PCM model. This again predicted a $\text{Mg}(\text{OH})_2$ cluster with two OH groups in the *trans* position. It is concluded that the stable species of the Mg(II) ion at pH = 10.5 is a neutral linear molecule of $\text{Mg}(\text{OH})_2$.

Dimerization Mechanism. As the next step, we examined the formation of a linked dimer, $[\text{Mg}(\text{OH})_2]_2$, from two $\text{Mg}(\text{OH})_2$ molecules in gas and water. Figure 2 shows the potential-energy curves along the Mg–Mg distance, $R_{\text{Mg-Mg}}$, with the other coordinates relaxed. We defined that the origin of the energy is twice the optimized energy of the monomer without water molecules, $\text{Mg}(\text{OH})_2$. The potential-energy curves indicate that a dimer product is generated with no energy barrier in both gas and water, while the dimerization energies are substantially different, that is, -3.43 eV in the gas phase and -2.19 eV in water. Though stabilization is smaller, it is concluded that dimerization spontaneously proceeds in water. The above observation is in contrast to the hydrolysis of Si–O–Si bonds of silicate minerals, which proceeds via an energy barrier.¹⁹ The equilibrium structure was obtained at $R_{\text{Mg-Mg}} = 0.291$ and 0.289 nm in gas and water, respectively, both of which are close to the experimental value of brucite (0.314 nm).³⁴ The angle of Mg–O–Mg ($A_{\text{Mg-O-Mg}}$) was 96.7 and 95.8° for the gas phase and a water solvent, respectively.

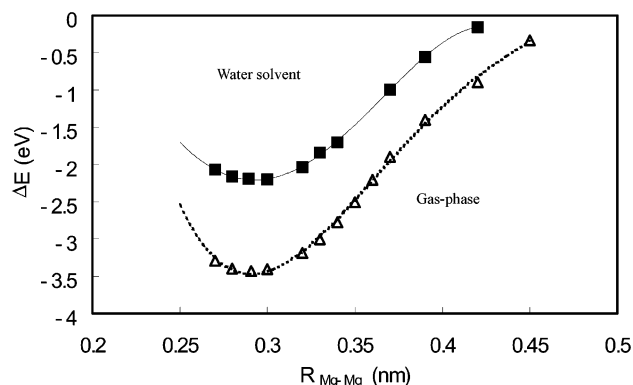


Figure 2. Potential energy curve of the dimerization reaction of $\text{Mg}(\text{OH})_2$ in either the gas phase (dotted curve) or a water solvent (solid curve) on $R_{\text{Mg-Mg}}$. The square and triangle symbols denote the calculated values in gas and water, respectively. As to the origin of the potential energy, the potential energy was set to 0 when two $\text{Mg}(\text{OH})_2$ molecules were separated at an infinite distance. The potential energy at that state was estimated to be equal to twice the calculated electronic energy of one $\text{Mg}(\text{OH})_2$. The curve for the water solvent was obtained using the PCM model.

(II) Formation of $[\text{Mg}(\text{OH})_2]_n$ Oligomers ($n > 2$) by a Hierarchical Approach. *Formation of Linked Trimers and Tetramers of $\text{Mg}(\text{OH})_2$ Molecules.* To examine the mineralization of $\text{Mg}(\text{OH})_2$, a similar optimization calculation was extended to a system consisting of 3–4 $\text{Mg}(\text{OH})_2$ molecules. First, $[\text{Mg}(\text{OH})_2]_n$ ($n = 2-4$) and $\text{Mg}(\text{OH})_2$ were placed at a nonbonding distance, and, thereafter, geometry optimization was performed in the gas phase and a water solution. This approach involving geometry optimization was performed by increasing the monomer number successively and can be called a hierarchical approach.

In the case of the trimer, $[\text{Mg}(\text{OH})_2]_3$, two optimized types were obtained in the gas phase, as are shown in Table 1. When the OH groups were classified by the number of their bridging Mg(II) ions, product a (denoted as trimer-product) had one OH group at a three-centered bridging position, three OH groups at two-centered bridging positions, and two OH groups at terminal edges, while product b (denoted as trimer-isomer) had three OH groups at two-centered positions and three OH groups at terminal edges. Trimer-product was 0.02 eV more stable than trimer-isomer. In trimer-product, three Mg(II) ions were located on the same plane. In a water solvent, only one product identical to trimer-product was obtained. The

(33) Pye, C. C.; Rudolph, W. W. *J. Phys. Chem. A* **1998**, *102*, 9933.

(34) Zigan, F.; Rothbauer, R. *Neues. Jahrb. Mineral., Monatsh.* **1967**, *4-5*, 245.

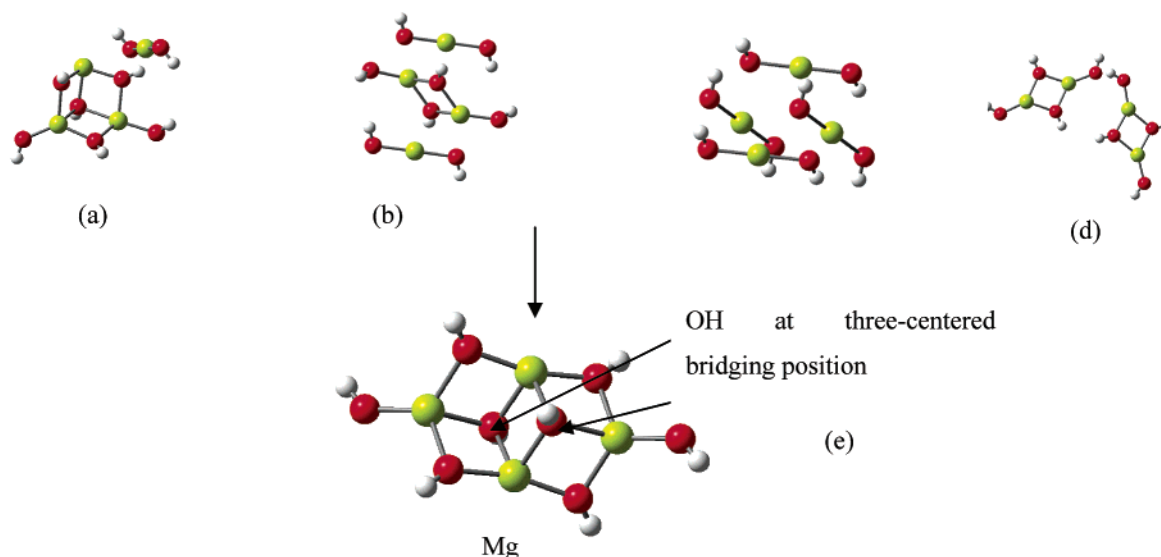


Figure 3. Formation of $[\text{Mg}(\text{OH})_2]_4$ in a gas phase, as was studied by the hierarchical method. (a) Initial state consisting of a trimer and one monomer. (b) Initial state consisting of a dimer and two monomers. (c) Initial state consisting of four monomers. (d) Initial state consisting of two dimers. (e) Calculated tetramer-product of $[\text{Mg}(\text{OH})_2]_4$.

Table 2. Comparison of the Interatomic Distances of Mg–Mg, Mg–O, O–O, and O–H in the Equilibrium Geometry of $[\text{Mg}(\text{OH})_2]_4$ of the Calculated and Experimental Results^{20,34}

distance (nm)	calculation	experimental
$R_{\text{Mg-Mg}}$	0.3000	0.3142
$R_{\text{Mg-O}}$	0.2020	0.2102
$R_{\text{O-O}}$	0.2650	0.2787
$R_{\text{O-H}}$	0.0960	0.0995

water solvent was taken into account as the PCM model. Trimer-product in a water solvent has one OH group at the three-centered bridging position, three OH groups at two-centered positions, and two OH groups at terminal edges. Thus, the presence of a water medium results in an increase of OH groups at the three-centered bridging positions.

In the case of a tetramer, $[\text{Mg}(\text{OH})_2]_4$, the following four initial states were assumed to see the effect of the initial structure on the final product: (1) one $\text{Mg}(\text{OH})_2$ molecule was added to the trimer, which had already been optimized (hierarchical approach), (2) two $\text{Mg}(\text{OH})_2$ molecules were added to the dimer, which had been optimized, (3) four $\text{Mg}(\text{OH})_2$ molecules were placed at the separated positions without any linkage, and (4) two dimers were placed at separated positions without any linkage. Figure 3a–e shows the reactants and products for these four initial structures in the gas phase. All of the initial states lead to the same product (tetramer-product) with two OH groups at the three-centered bridging positions, four OH groups at the two-centered bridging position, and two OH groups at the terminal edges. In this product, all of the Mg(II) ions are nearly on the same plane with the average distance of $R_{\text{Mg-Mg}}$ being ~ 0.3 nm. Table 2 summarizes the calculated equilibrium geometry of $[\text{Mg}(\text{OH})_2]_4$ in tetramer-product. The calculated interatomic distances agree well with the experimental data for brucite.^{20,34}

The initial relative orientation between two reacting dimers was chosen in a wide range with the purpose of examining the uniqueness of tetramer-product. The second row of Table 3 gives four selected initial positions, each of which is characterized by the dihedral angle between planes made by two $[\text{Mg}(\text{OH})_2]_2$ moieties. The geometry was optimized with no restraint on positions and angles.

After optimization, the final products were obtained as shown in the first row of Table 3. Two isomers, isomer-1 and isomer-2, have coplanar Mg(II) ions, while one, isomer-3, has a cubic shape. The third row of the table gives the difference in the energy with respect to tetramer-product. As a result, tetramer-product is found to be the most stable among these isomers. Clusters of tetramer-product, isomer-1, and isomer-2 constitute a partial structure of brucite crystal. Comparing the structures of these isomers with a focus on the nature of the OH groups, the presence of three-centered bridging OH groups, as it is displayed in the last three rows of Table 3, is essential for stabilizing a cluster and for creating a layered structure.

Formation of Higher Oligomers, $[\text{Mg}(\text{OH})_2]_n$ ($n > 4$). The structure of $[\text{Mg}(\text{OH})_2]_n$ ($n = 5-10$) was calculated basically in a manner similar to the formation of tetramer-product from trimer-product and a monomer. The geometry optimization of $[\text{Mg}(\text{OH})_2]_n$ was performed for a system of a $\text{Mg}(\text{OH})_2$ monomer and a $[\text{Mg}(\text{OH})_2]_{n-1}$ oligomer. An initial state for optimization was selected as follows: $\text{Mg}(\text{OH})_2$ was arbitrarily placed at the vicinity of $[\text{Mg}(\text{OH})_2]_{n-1}$. The distance between a Mg(II) ion in $\text{Mg}(\text{OH})_2$ and the nearest Mg(II) ion in $[\text{Mg}(\text{OH})_2]_{n-1}$ was kept at 0.3–0.5 nm to avoid bond formation. The initial orientation of $\text{Mg}(\text{OH})_2$ was changed by rotating its Mg(II)–O bond around the axis connecting the Mg(II) ion in $\text{Mg}(\text{OH})_2$ and the nearest Mg(II) atom in $[\text{Mg}(\text{OH})_2]_{n-1}$. The dihedral angle between $[\text{Mg}(\text{OH})_2]$ and the molecular plane of the $[\text{Mg}(\text{OH})_2]_{n-1}$ monomer was changed from 90 to 180°. Calculations were performed for 4–8 cases as an initial position. Structure optimization for a system of $\text{Mg}(\text{OH})_2$ and $[\text{Mg}(\text{OH})_2]_{n-1}$ was performed by minimizing the total energy with respect to all degrees of freedom, for example, bond lengths, bond angles, and dihedral angles.

We found two or three isomers as an optimized structure of an oligomer ($[\text{Mg}(\text{OH})_2]_n$). By comparing the total energy among these isomers, the most stable isomer was always a planar product consisting of a fused structure of a stable trimer-product (Table 1, a). In one case, an isomer possessed an unstable trimer-isomer (Table 1, b) as a partial structure. This kind of isomer was unstable in comparison to the planar isomer. In another type of isomer, the terminal OH group was oriented differently from the

Table 3. Total Energies and Other Characteristics for Possible Isomers Including Four Mg Atoms^{a,b}

Isomers	(a)tetramer-product in Fig. 3 (e)	(b)isomer-1	(c)isomer-2	(d)isomer-3
Initial of two dimers four Mg dihedral angle (°)	25	45	180	60
ΔE (eV)	0	+1.15	+1.33	+0.613
No. of OH's at three-centered bridging positions	2	1	0	0
No. of OH's at two-centered bridging positions	4	4	6	4
No. of OH's at terminal edges	2	3	2	4

^a ΔE = total optimized energy; optimized energy (tetramer-product) in Figure 3e. ^b (b–d) Optimized isomers from two dimers, which were obtained from various initial positions.

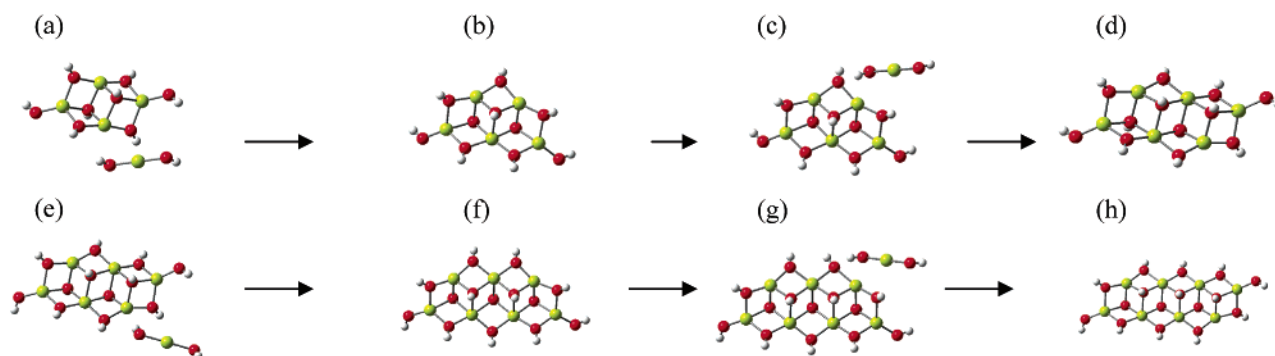


Figure 4. Formation of $[\text{Mg}(\text{OH})_2]_n$ ($n = 5-8$) in a gas phase, as studied by the hierarchical method. (a) Initial state consisting of tetramer-product and one monomer. (b) Calculated pentamer-product of $[\text{Mg}(\text{OH})_2]_5$. (c) Initial state consisting of pentamer-product and one monomer. (d) Calculated hexamer-product of $[\text{Mg}(\text{OH})_2]_6$. (e) Initial state consisting of hexamer-product and one monomer. (f) Calculated heptamer-product of $[\text{Mg}(\text{OH})_2]_7$. (g) Initial state consisting of heptamer-product and one monomer. (h) Calculated octamer-product of $[\text{Mg}(\text{OH})_2]_8$.

most stable isomer. Because the energy difference due to the rotation of an OH group was negligible, these isomers were not differentiated. Other types of isomers were not obtained when a higher oligomer was optimized by the present hierarchical approach.

Figure 4 summarizes the initial states and products for the formation of $[\text{Mg}(\text{OH})_2]_n$ ($n = 5-8$). In all of these structures, Mg(II) ions in the products are nearly on the same plane, indicating that a linked $[\text{Mg}(\text{OH})_2]_n$ cluster reaches a layered structure spontaneously.

As for a nanomer or a decamer, their structures were also calculated by starting a reaction of octamer-product or nanomer-product with a monomer, respectively. These calculations predicted the layered optimized structure, which is summarized in Table 4. These calculations were also confirmed by starting a reaction of tetramer-product with pentamer-product or with hexamer-product. It was, thus, confirmed that the coplanar structure, as is shown in Figure 4 and Table 4, is a unique product of each oligomer, irrespective of the choice of the initial reactants.

Formation Energy of $\text{Mg}(\text{OH})_2$ Clusters. Figure 5 shows the dependence of the stabilization energy of a cluster on the size of a cluster. The stabilization energy of a cluster is defined by $\Delta E/n$, where n is the total number of monomer

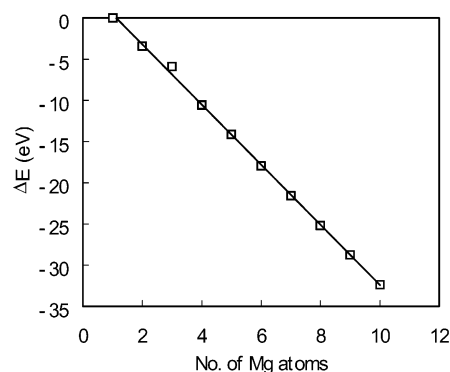


Figure 5. Dependence of the calculated stabilization energy calculated by eq 2 for $[\text{Mg}(\text{OH})_2]_n$ ($n = 1-10$) on the number of Mg atoms.

units in a cluster and ΔE is the energy difference of the following reaction:



$$\Delta E = E(\text{product}) - E(\text{reactant}) \quad (2)$$

where $E(\text{product})$ is the optimized total energy for a given oligomer and $E(\text{reactant})$ is the sum of n times the energy

Table 4. Summary of the Characteristics for the Products of the Nanomer and Decamer

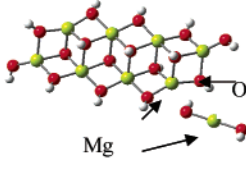
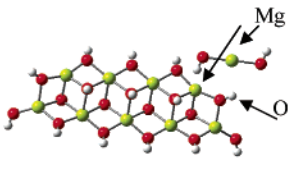
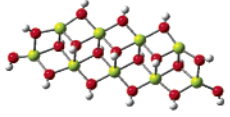
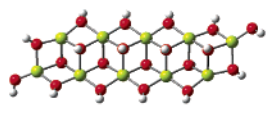

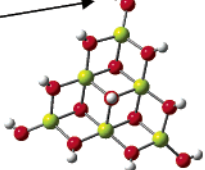
oligomer	nanomer	decamer
Initial structure		
	Mg-Mg(monomer) 0.38 nm Mg-O-Mg(monomer) 100 °	Mg-Mg(monomer) 0.38 nm Mg-O-Mg(monomer) 77 °
Product		
No. of OH's at three-centered bridging positions	7	8
No. of OH's at two-centered bridging positions	9	10
No. of OH's at terminal edges	2	2

Table 5. Summary of the Characteristics of the Trimer and Hexamer with a Free OH⁻ Group

Product	(a) trimer-OH product	(b) hexamer- OH product
		
Initial cluster	dimer, monomer, OH ⁻	pentamer, monomer, OH ⁻
No. of OH's at three-centered bridging positions	1	4
No. of OH's at two-centered bridging positions	3	6
No. of OH's at terminal edges	3	3

of the optimized monomer. $\Delta E/n$ corresponds to the stabilization energy per one Mg(II) cation caused by the formation of Mg–O–Mg bridges. As is shown in the figure, the stabilization energy increases in proportion to the number of Mg(OH)₂ monomers. It is, thus, expected that the larger the number of Mg–O–Mg bridges is, the more stabilized the oligomer is. This finding allows us to substantiate the earlier hypotheses that the Mg–O–Mg linkage of Mg atoms should not be a rate-determining step for the mineralization of a single layer. When the structures of the oligomers were compared, as is shown in Figure 4, the enhancement of the stability along with an increase in the cluster size seemed to lie in the increased number of OH groups at the three-centered bridging positions. In fact, the number of such OH groups increases to three (pentamer), four (hexamer), five (heptamer), six (octamer), seven (nanomer), and eight (decamer).

Effect of Free Hydroxyl Anions on Cluster Formation. To examine the possibility that free OH⁻ ions participated in the formation of a [Mg(OH)₂]_n cluster, the structure

optimization of a trimer was performed in the gas phase by adding one OH⁻ ion to the system of an optimized dimer and one monomer. Table 5 gives an optimized structure of such a trimer with its characteristics. It has a highly symmetric structure with one OH group at a three-centered bridging position, three OH groups at two-centered bridging positions, and three OH groups at terminal edges. Thus, the participation of free OH⁻ ions leads to the formation of a stable anionic cluster.

The effect of a free OH⁻ ion was examined for the formation of a hexamer, [Mg(OH)₂]₆. For that purpose, the final product was optimized by reacting pentamer-product, [Mg(OH)₂]₅, with Mg(OH)₂ in the absence or presence of a free OH⁻ ion. In the absence of OH⁻, hexamer-product (as was already shown in Figure 4d) was obtained. To the contrary, in the presence of free OH⁻, an anionic cluster, [Mg₆(OH)₁₃]⁻, was derived, as given in Table 5. It should be noted that [Mg₆(OH)₁₃]⁻ is a triangular-shaped cluster with four three-centered OH⁻ groups, while hexamer-product is a rectangular-shaped cluster with four

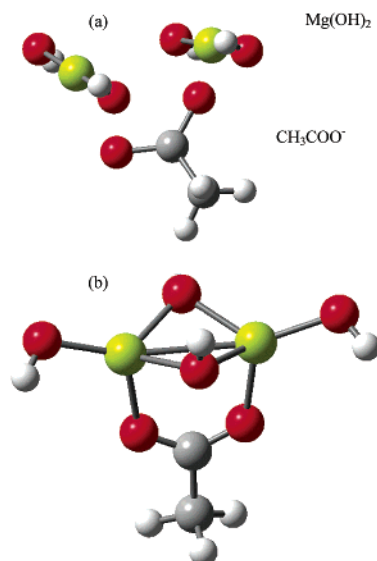


Figure 6. Dimerization of $\text{Mg}(\text{OH})_2$ in the presence of an acetate ion. (a) Initial state of two monomers with an acetate ion. (b) Geometrically optimized state of $[\text{Mg}(\text{OH})_2]_2$ linked to an acetate ion.

three-centered OH^- groups. Thus, the participation of free OH^- ions may have an effect on the shape of a stable cluster.

(III) Templating Effect by an Acetate Ion. *Templating Effect for Dimerization.* In our previous work,¹⁷ a stearate monolayer acted as a template for the formation of brucite at an air–water interface. Deprotonated carboxyl groups in the monolayer orient toward a water phase. At an initial step, such carboxylate groups might bind $\text{Mg}(\text{OH})_2$ molecules to accelerate the rate of polymerization. To obtain theoretical support for such a mechanism, the dimerization reaction of $\text{Mg}(\text{OH})_2$ was studied in the presence of an acetate ion. Here, an acetate ion was assumed to represent a polar group of a stearate monolayer. The initial structure was assumed to consist of two separated $\text{Mg}(\text{OH})_2$ molecules and an acetate ion (CH_3COO^-) in the water phase, as is shown in Figure 6a. Optimization was performed under no constraint. In the optimized structure, as is shown in Figure 6b, two oxygen atoms of an acetate ion are linked to the two Mg atoms. This bridging resulted in a decrease of the distance between two Mg atoms ($R_{\text{Mg-Mg}}$) from 0.291 nm (Figure 2) to 0.278 nm. The stabilization energy due to the acetate ion is defined as follows:

$$\Delta E = \Delta E_1 - \Delta E_2 \quad (3a)$$

$$\Delta E_1 = E(\text{a dimer connected to an acetate ion}) - E(\text{two monomers and an acetate ion}) \quad (3b)$$

$$\Delta E_2 = E(\text{a dimer}) - E(\text{two monomers}) \quad (3c)$$

According to eq 3, the stabilization energy by an acetate ion to form a dimer was estimated to be -3.52 eV.

In experiments, it was shown that brucite was formed more rapidly under a stearate monolayer than in a homogeneous solution.¹⁷ Although the above calculation did not take into account the desolvation of a carboxylate group, it is suggested that the coordination of the $\text{Mg}(\text{II})$ ion increases the rigidity of the monolayer and that the polymerization of $\text{Mg}(\text{OH})_2$ is accelerated by the carboxyl groups of a stearate monolayer.

Significance of the Present Calculation in Template Mineralization. When the results of the present calculation are extrapolated to the system of an infinite number of $\text{Mg}(\text{OH})_2$ molecules or brucite crystal, we are led to the hypothesis that the layered structure of brucite is a natural consequence of the linkage reaction. As is evidently shown by the reaction path studies (Figure 2), there is no energy barrier in the linkage process. Such a layered structure is expected to be formed whether it takes place in a homogeneous solution or underneath a template monolayer. Thus, a key process for preparing a thin film of brucite would be how the crystal growth normal to a layer surface is inhibited to reduce the film thickness. In fact, the effect of an inhibitor on the film thickness has been noted in other kinds of mineralization experiments.^{8–13} Calcite formation under a biomimetic floating monolayer, for example, exhibited a remarkable effect of an anionic polymer on film morphology.⁹

The presence of an acetate ion is shown to stabilize the dimer formation of $[\text{Mg}(\text{OH})_2]_2$. If a similar effect is expected under a stearate monolayer, it will explain the observed templating effect of a stearate monolayer in accelerating the formation rate of brucite.¹⁷

Conclusion

In this work, we applied quantum chemical ab initio methods to study the mineralization of $\text{Mg}(\text{OH})_2$ under a monolayer template. As a first step to this goal, we studied the structures and reactions of brucite. Theoretical studies have postulated that (I) the formation of a Mg-O-Mg bridge during dimerization of two $\text{Mg}(\text{OH})_2$ molecules proceeded with no potential barrier and (II) that a solvent has little effect on the reaction path of mineralization. It has been confirmed that brucite exists intrinsically as a layered structure. Besides, the presence of an acetate ion stabilizes the dimer structure of $\text{Mg}(\text{OH})_2$ as a result of the bridge between two Mg atoms. These results are important concerning how to explore the templating system to prepare a large thin crystal of LDHs in the future.

Acknowledgment. We thank Prof. Kogure (the University of Tokyo) for his valuable discussion. This work was financially supported by a Grant-in-Aid for Scientific Research on Priority Areas (417) from the Ministry of Education, Culture, Sports, Science and Technology (MEXT) of the Japanese Government. This work has been supported by CREST of JST (Japan Science and Technology Corporation).

LA034546L